Chapter 4. Stepwise auroral substorm evolution observed by meridian scanning photometers at Syowa and Asuka stations in 1989

4.1. Purpose of this Chapter

Purpose of this Chapter is to show how many events, which had similar characteristics as shown in the Chapter 3 for the special event on June 6-7, 1989, were observed by the auroral observation at Syowa and Asuka stations during the whole observation period in 1989. Observations by the meridian scanning photometer (MSP) are especially focused on.

4.2. Features of the auroral substorm evolution in the event on June 6-7, 1989

The features observed by the MSP in the special event are schematically summarized in the Figure 4.1. Fig. 4.1(a) shows the auroral substorm evolution in the invariant latitude (ILAT) vs time plot. Electron auroral emission region is shown with shaded area, and latitudinal range of the proton auroral emission region is shown with thick broken lines. Several timings are indicated with upward arrows below the time axis. Tg marks the start time of the equatorward motion of auroral oval, indicating the start of the growth phase; Ton is the time of the expansion phase onset of the substorm; T0 is the start time of the poleward expansion at the station; T1 is the time when the initial poleward expansion is apparently slowed, or the poleward expansion reached a ceiling latitude; T2 is the time when a further poleward expansion apparently starts. We call the period from T0 to T1 the Stage-1, from T1 to T2 the Stage-2, and after T2 the Stage-3. Hence the local auroral poleward expansion proceeded in a stepwise fashion with those three distinct stages, which is one of the most stressed observational results in the detailed study in the Chapter 3.

The period from Tg to T0 is a local growth phase. During the local growth phase, two characteristic auroral activities were observed, the FEM arc and the NPSBL aurora. The FEM arc appeared around the poleward boundary of the auroral oval, which is indicated with a thin dotted line in Fig. 4.1(a), and it moved equatorward toward the proton main oval on the equatorward side. The equatorward motion of the FEM arc was slowed as it approached the proton main oval, and eventually it was located around the poleward edge of the proton main oval just before T0. The NPSBL aurora clearly appeared around the poleward boundary when the FEM arc approached the proton main oval. It appeared before the global onset time Ton, and continued to exist around the poleward boundary even after Ton. The ceiling latitude of the Stage-1 to Stage-2 was very close to the latitude of the NPSBL aurora. A further poleward expansion during the Stage-3 started with a significant intensification of the higher latitude side of the NPSBL aurora. In other words, the NPSBL aurora always marks the poleward boundary of the auroral oval. This NPSBL aurora is supposed to be one of the most important findings in our study. Such a close association of the evolution of the NPSBL aurora with the local stepwise evolution suggests that the local poleward expansion should be closely related with the evolution of the NPSBL aurora.

During the period from the Stage-1 to the Stage-2, the proton auroral emission coexisted with the electron auroral emissions. After the Stage-3 started, the electron auroral emission region was bifurcated into the poleward expanding part and the equatorward moving part, and the proton

auroral emission on the equatorward side gradually became weak. Such a proton auroral fading started from the most-equatorward side and spread to higher latitudes. On the equatorward side, the electron auroral emission region became diffuse, and the pulsating auroral activity started to appear within it.

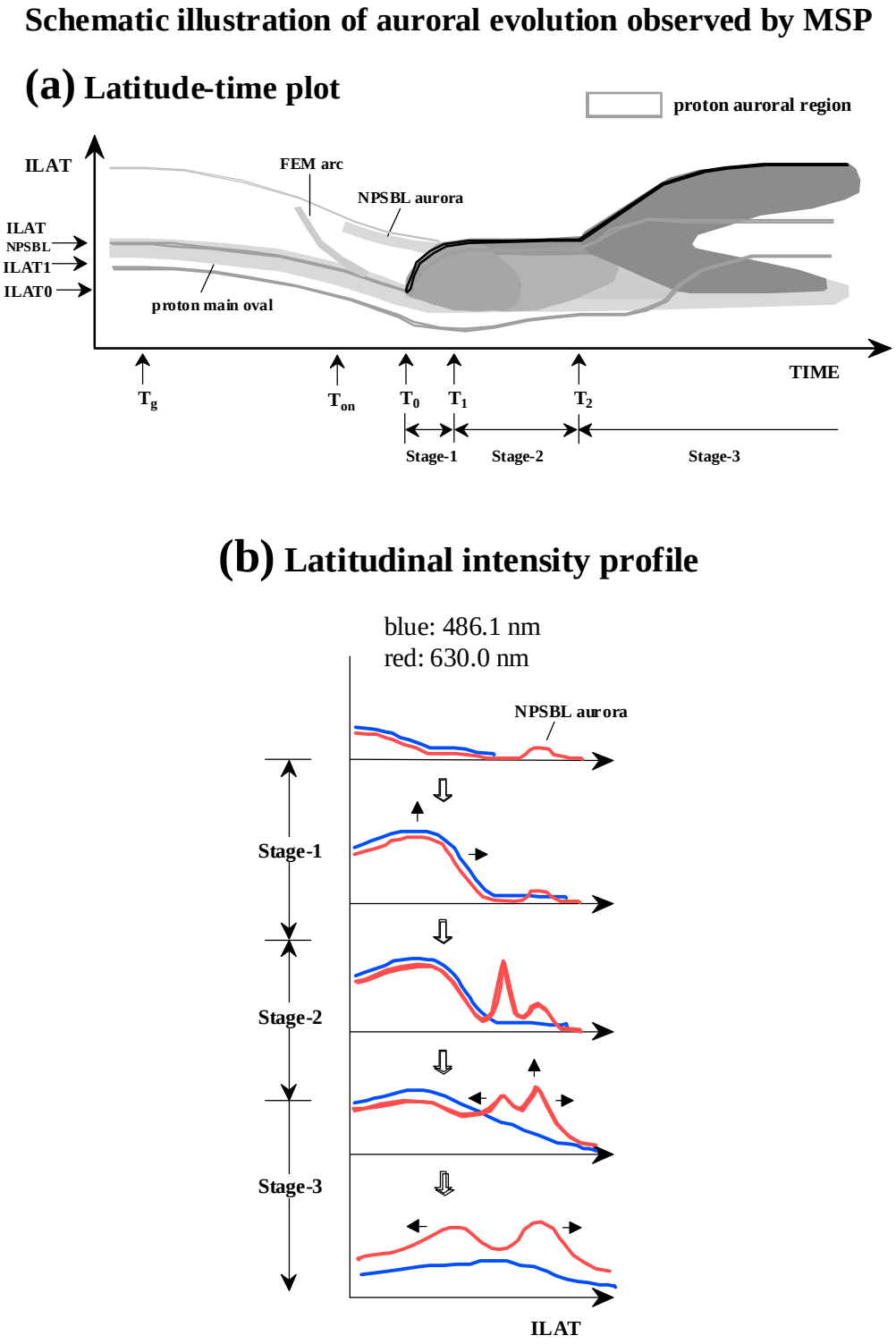

Figure 4.1. Schematic summary of the auroral substorm features observed by the MSP in the special event on June 6-7, 1989, which was analyzed in detail in Chapter 3. Evolution in the ILAT-time plot (a) and of the latitudinal intensity profile (b).

Such an evolution of the proton and electron auroras during the period from the Stage-1 to the Stage-3 is schematically shown in Fig. 4.1(b). Each panel in Fig. 4.1(b) shows the latitudinal intensity profiles of the proton (blue line) and electron (red line) auroral emissions, and the time advances downward. The Stage-1 is characterized by the rapid poleward expansion both of the proton and electron main auroral regions up to the latitudes of the NPSBL aurora. During the Stage-2, intense electron auroral activities appeared around the interface region between the NPSBL aurora and the equatorward-side main auroral region. The Stage-3 started with a significant intensification of the higher latitude side of the NPSBL aurora, which resulted in the bifurcation of the electron emission region. The proton auroral emission was significantly reduced, especially in the equatorward region.

4.3. Event selection and analysis procedure

As described in the Chapter 2, the auroral observation by the MSP was carried out in the total 56 nights at Syowa station, and in the 104 nights at Asuka station during the wintertime in 1989. The total 30 and 58 events, where an apparent equatorward motion of the proton main oval followed by a sudden apparent poleward expansion was observed, were selected by the eye-inspection of the latitude-time plot for the Syowa and Asuka MSP data, respectively. As described in the Chapter 2, those 88 events were categorized into three types, the TYPE-1, TYPE-2, and TYPE-3. We have checked that the characteristic features, observed in the event on June 6-7, can also be seen in those 88 events. Table 4.1 lists the result. The event on June 6-7 is categorized in the TYPE-2.

Table 4.1. Summary of the MSP observation for poleward expansion event in 1989

expansion type	total no	NPSBL aurora	FEM arc	proton fade	3stage	bifur-cation	NPSBL & 3stage	NPSBL & 3stage & good data	NPSBL & no3stage	NPSBL & no3stage &bifurcation
TYPE-1	41	16 (39%)	5 (12%)	25 (61%)	4 (10%)	36 (88%)	4 (10%)	4	12	12
TYPE-2	32	22 (69%)	11 (34%)	18 (56%)	22 (69%)	28 (88%)	14 (44%)	13	8	4
TYPE-3	15	1 (7%)	1 (7%)	4 (27%)	0 (0%)	11 (73%)	0 (0%)	0	0	0
total	88	39	17	47	26	75	18	17	20	16

expansion type	noNPSBL & 3stage	noNSPBL & no3stage	noNPSBL & no3stage & bifurcation	3stage & bifurcation	no3stage & bifurcation	bifurcation & proton fade
TYPE-1	0	25	21	3	33	25
TYPE-2	8	2	2	22	6	18
TYPE-3	0	15	11	0	11	4
total	8	42	34	25	50	47

Table 4.1 shows that the NPSBL aurora was observed before T0 in 39 %, 69 %, and 7 % of the total events for the TYPE-1, TYPE-2, and TYPE-3, respectively. Hence the NPSBL aurora can be

observed with a high probability in the case of the TYPE-2. Figure 4.2 (b) shows the location of the initial poleward expansion at T0 when the NPSBL aurora was observed. The NPSBL aurora appeared in the TYPE-1 events, when the initial poleward expansion occurred around the midnight local times and at lower latitudes.

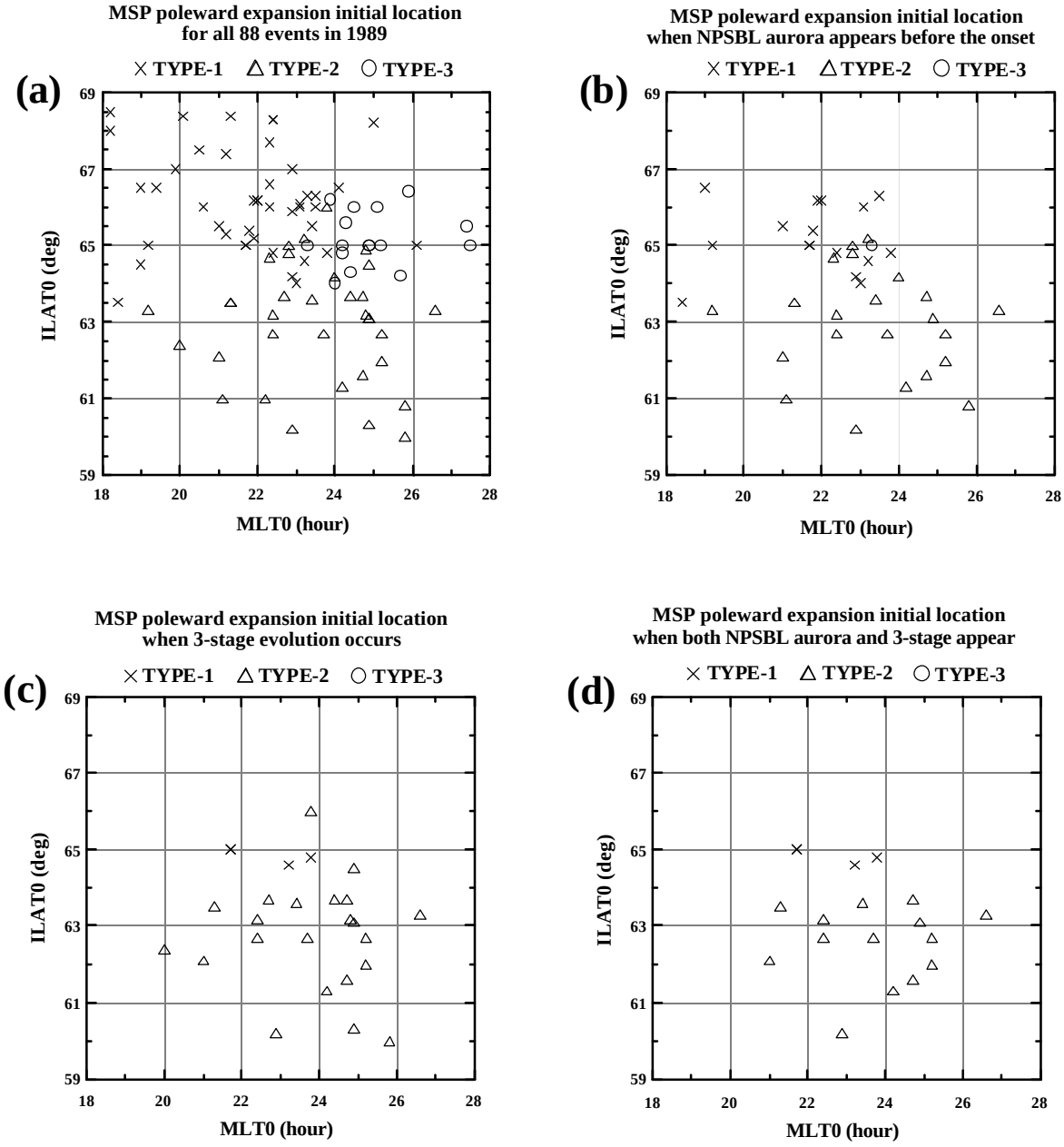

Figure 4.2. Distribution of the start location of the initial poleward expansion for the total 88 events (a), for the events with the NPSBL aurora (b), for the events with three-stage evolution (c), and for the events both with the NPSBL aurora and the three-stage evolution (d). Cross, triangle, and circle symbols correspond to the expansion type of TYPE-1, -2, and -3, respectively.

Identification of the FEM arc only from the MSP data is rather difficult, but Table 4.1 shows that the FEM arc can be observed with a highest probability in the case of the TYPE-2. The

three-stage evolution, as shown in Fig. 4.1(a), can be also observed with a highest probability in the case of the TYPE-2, and was not observed at all in the case of TYPE-3. Figure 4.2 (c) shows the location of the initial poleward expansion, when the three-stage evolution was observed. It can be seen that the initial poleward expansion occurred around the midnight local times at lower latitudes. Figure 4.2 (d) shows the location of the initial poleward expansion, when both the NPSBL aurora and the three-stage evolution appeared.

The bifurcation of the bright electron auroral region after the poleward expansion was observed with a high probability in all the expansion types. In the case of the TYPE-1 and TYPE-3, most of the bifurcation occurred without the three-stage evolution.

The fading of the proton auroral emission after the poleward expansion was observed with a high probability in the case of TYPE-1 and TYPE-2. It is rather difficult to distinguish the fading from the smooth poleward shift of the proton auroral region after the poleward expansion in the case of the TYPE-3. The fading of the proton auroral emission always occurred after the bifurcation of the electron auroral region. There were no cases where the fading occurred without the bifurcation.

There were 8 events where the three-stage evolution was observed without the NPSBL aurora before T0. In all the 8 events, the characteristics of the three-stage evolution were very similar to those for the evolution with the NPSBL aurora.

In summary, the characteristic features, which were observed in the event on June 6-7, 1989, can be observed with a high probability when the initial poleward expansion occurred around the midnight local times at lower latitudes. The characteristics of the poleward expansion at earlier or later local times and at higher latitudes were different from those around midnight at lower latitudes, which suggests that some different processes should proceed in the magnetospheric region corresponding to such locations.

Next we concentrate on the events, where both the three-stage evolution and the NPSBL aurora were observed in the case of the TYPE-2. The total number of such "good" events was 13. Table 4.2 lists the details of those 13 events. In Table 4.2, ILAT0, ILAT1, $ILAT_{NPSBL}$ are the latitudes where the initial poleward expansion starts at T0, the ceiling latitude of the Stage-1 at T1, and the latitude of the NPSBL aurora at T0, respectively. We defined these latitudes with the location of the maximum intensity of the 486.1 nm emission for ILAT0 and ILAT1, and the highest latitude of the local maximum intensity of the 630.0 nm emission for the $ILAT_{NPSBL}$, respectively. MLT0 in Table 4.2 is the magnetic local time of the station at T0.

Figure 4.3 shows the data for the event 4, which is the special event analyzed in detail in the Chapter 3. Fig. 4.3(a) is a plot in a longer time scale showing the whole period of the growth phase, and Fig. 4.3(b) is an expanded plot showing the details of the expansion phase evolution. White vertical lines in each panel indicate the timings which we determined.

Figure 4.4 shows locations of the local maximum (Fig. 4.4(a)) and the maximum (Fig. 4.4(b)) of the 486.1 nm emission in each meridian scan from 23:20:00 UT on June 6 to 01:20:00 UT on June7, 1989 in the event 4. Comparing with Fig. 4.3(a), the trend of the lower latitude part of the local maximum locations and the trend of the maximum locations in Fig. 4.4 follow the

equatorward motion of the proton main oval. We determined the time Tg as the start time of the equatorward shift of the most-equatorward point of the local maximum locations in the trend.

Table 4.2. Auroral poleward expansion event observed by the MSP at SYOWA and ASUKA stations in 1989

event no	T0 (UT) proton aurora m/dd		T0-Tg station hh:mm:ss arc	fade	T0-Ton (min)	T1-T0 (min)	T2-T0 (min)	MLT0 (min)	ILAT0 (hour)	ILAT1 (deg)	ILAT (deg)	NPSBL NPSBL		FEM
1.	4/04	21:47:13	29.8	15.2	2.0	15.9	21.0	62.0	65.8	65.6	y		y	A
2.	5/01	21:53:08	23.0		1.5	5.5	21.3	63.5	64.5	65.3	y		y	A
3.	6/07	00:52:15	69.3	10.0	2.5	9.0	24.2	61.3	64.0	66.8	y	y	y	A
4.	6/07	00:55:31	75.5	13.3	3.5	8.0	25.2	62.0	64.4	66.7	y	y	y	S
5.	6/07	22:58:13	95.6		2.0	12.5	22.4	63.2	63.7	65.9	y	y	y	A
6.	6/07	23:04:45	103.6		5.5	15.0	23.4	63.6	65.1	66.1	y	y	y	S
7.	6/14	03:17:56	67.6	17.9	3.0	17.5	26.6	63.3	65.0	66.5	y		y	A
8.	8/10	01:39:58	75.6	3.0	1.0	9.0	24.9	63.1	64.3	65.2	y		y	A
9.	8/11	01:26:13	55.5	4.7	1.0	15.0	24.7	61.6	63.3	66.4	y	y	y	A
10.	8/27	23:08:43	57.1	20.7	2.5	5.5	22.4	62.7	64.9	66.5	y		y	A
11.	9/04	00:33:06	51.6	6.6	5.0	25.5	23.7	62.7	64.6	66.9	y		n	A
12.	9/04	00:35:34	54.0	9.1	8.5	25.5	24.7	63.7	65.0	67.4	y	y	n	S
13.	9/05	01:56:34	71.6	22.6	5.5	20.0	25.2	62.7	65.2	67.3	y		n	A

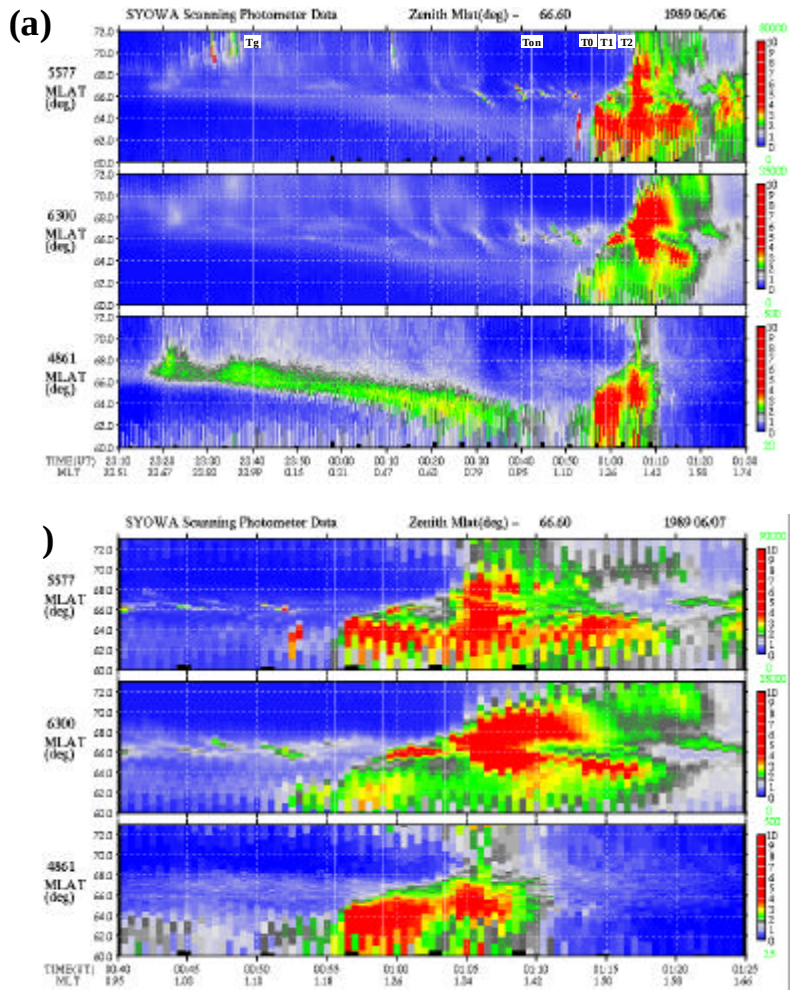

Figure 4.3. MSP data for the event 4 in the Table 4.2. ILAT-time plots of three auroral emissions are shown in a longer time scale (a) and in a shorter time scale (b). White vertical lines in each panel indicate timings which are shown in Fig. 4.1(a).

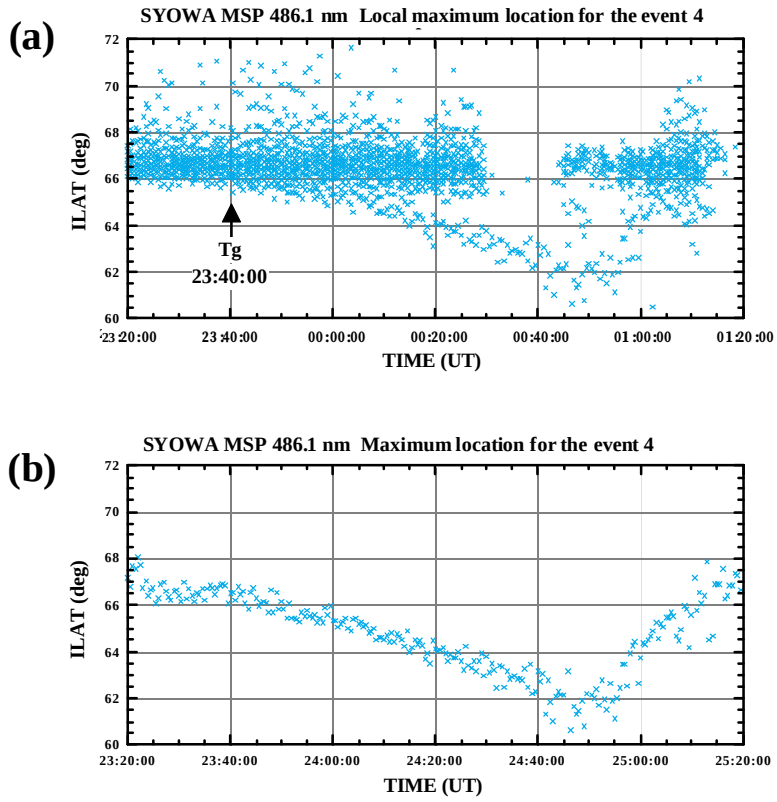

Figure 4.4. Location of the local maximum (panel (a)) and the maximum (panel (b)) of the 486.1 nm emission from 23:20:00 UT on June 6 to 01:20:00 UT on June7, 1989 in the event 4.

Figure 4.5 shows how we determined the time T0, T1, and T2. Each panel from top in Fig. 4.5 shows the time evolution from 00:40:00 UT to 01:20:00 UT on June 7, 1989 for the maximum intensity at each meridian scan (panel (a)), the ILAT at the time of the maximum intensity (panel (b)), the local maximum location for the 630.0 nm emission (panel (c)) and the 486.1 nm emission (panel (d)), respectively. In panel (a) and (b), the black, red, and blue dots and lines show the data for the 557.7, 630.0, and 486.1 nm emissions, respectively. We determined the time T0 with an apparent increase of the maximum intensity in panel (a) and an apparent start of the poleward shift of the maximum intensity location for the 486.1 nm emission in panel (b). The time T1 was determined with the termination of the poleward shift of the location and an apparent poleward jump of the maximum location of the 630.0 nm emission, in panel (b). The time T2 was determined with an apparent increase of the maximum intensity for all the wave lengths in panel (a). This timing nearly corresponds to the start of the further poleward spread of the local maximum locations of both the 630.0 nm and 486.1 nm emissions in panel (c) and (d), respectively. $ILAT_{NPSBL}$ was determined as the latitude of the highest point of the local maximum locations at T0 for 630.0 nm emission in panel (c). The existence of the NPSBL aurora can be rather clearly identified with such a local maximum plot as panel (c).

The existence of the FEM arc is rather difficult to be identified only from the ILAT-time plot of the MSP as shown in Fig. 4.3(a). For this event, the FEM arc could be identified more clearly in

the MSP data at Asuka station as described in Chapter 3, and the all-sky SIT-TV data at Syowa station was very essential for the identification. The blanks in the column for the FEM arc identification in Table 4.2, hence, indicate that we cannot say definitely whether the FEM arc exists or not only from the MSP data.

The weakening or fading of the proton auroral emission after T2 is easier to be identified, as shown in Fig. 4.3(a) and (b). Such a fading can also be seen in the local maximum plots in the panel (d) in Fig. 4.5.

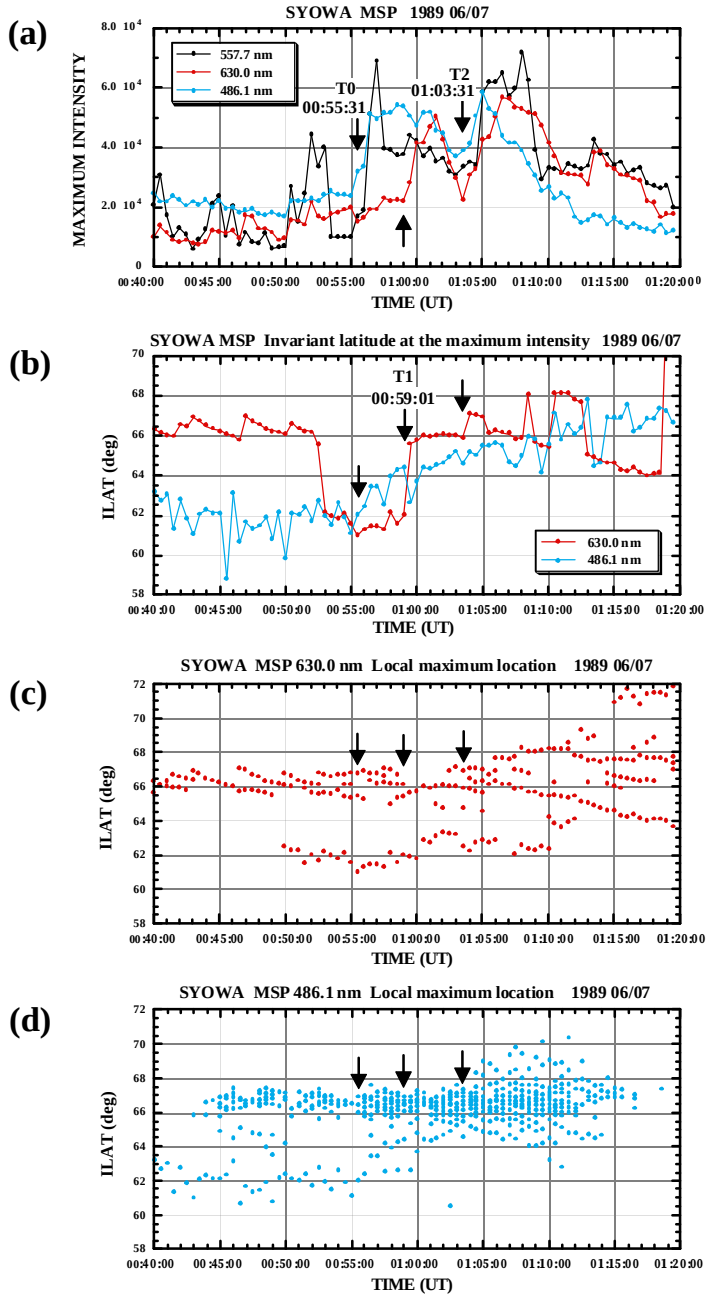

Figure 4.5. (a) Evolution from 00:40:00 UT to 01:20:00 UT on June 7, 1989 of the maximum intensity in each meridian scan. (b) ILAT of the maximum intensity. (c) Local maximum location of the 630.0 nm emission. (d) Local maximum location of the 486.1 nm emission. In the panel (a) and (b), black, red, and blue dots and lines show the 557.7, 630.0, and 486.1 nm emissions, respectively.

The time of the expansion phase onset, Ton, is determined with the magnetograms at the low and mid-latitude stations which are located in the midnight sector during the MSP observation. We searched the start both of the magnetic bays in the H and D components and the Pi2 pulsations. Ton could be rather clearly determined in the 7 events. In other 6 events, it was rather difficult to determine the onset time definitely. In the 7 events, the local initial poleward expansion occurred well after the global expansion phase onset. Hence the local poleward expansion in the 7 events should occur as a result of the azimuthal expansion of the global auroral disturbance region (auroral bulge), as shown in the Chapter 3 for the event 3 and 4.

4.4. Selected examples

Five more examples selected from the 13 events are shown in Figure 4.6(a)-(e). Fig. 4.6(a) to (e) are for the events 2, 3, 7, 9, and 12, respectively. White lines in each panel indicate the times, Tg, Ton, T0, T1, and T2, which were determined with the same procedure as described in the section 4.2. The NPSBL aurora can be identified in each panel, more clearly in the panel for 630.0 nm emission. The FEM arc can be seen in Fig. 4.6(b) and (d), and less clearly in Fig. 4.6(e). In all the three events, the FEM arc appeared around the poleward boundary, and moved equatorward toward the proton main oval. Its equatorward motion started before the expansion phase onset Ton. In the events 9 and 12, the NPSBL aurora can be identified before Ton, as in the case of the event 3 and 4. For the event 12, the all-sky SIT-TV data at Syowa station were available, and we can see the two-dimensional features of the FEM arc and the NPSBL aurora, as in the case of the event 3 and 4. In the events 2, 3, 7, and 9, the proton auroral emission became weak after the bifurcation of the electron auroral region after T2. Such a proton auroral fading started from lower latitudes and then spread to higher latitudes. In contrast, in the event 12, the proton auroral emission in the lower latitudes continued to be enhanced even after T2.

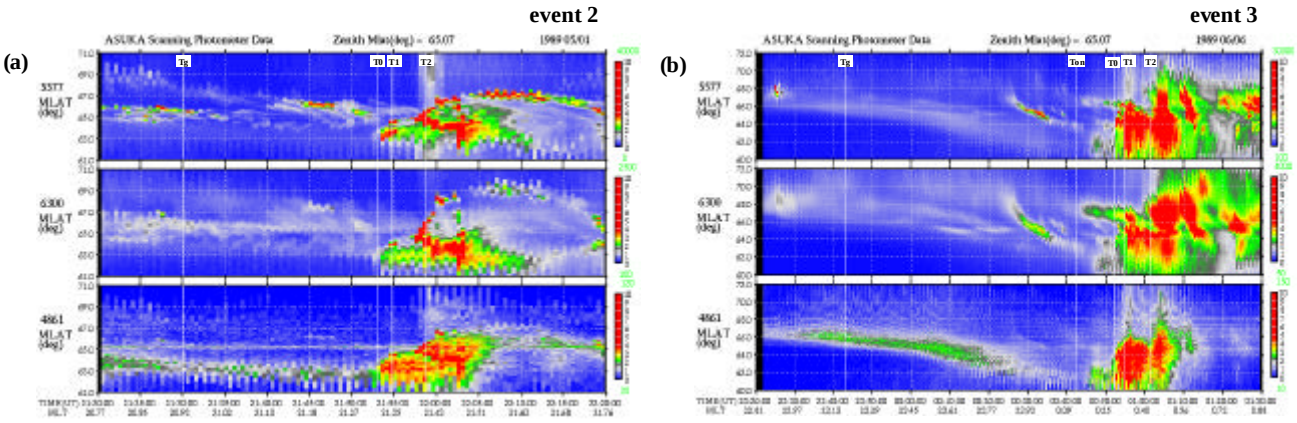

Figure 4.6. ILAT-time plot of the MSP data for the event 2 (a) and the event 3 (b).

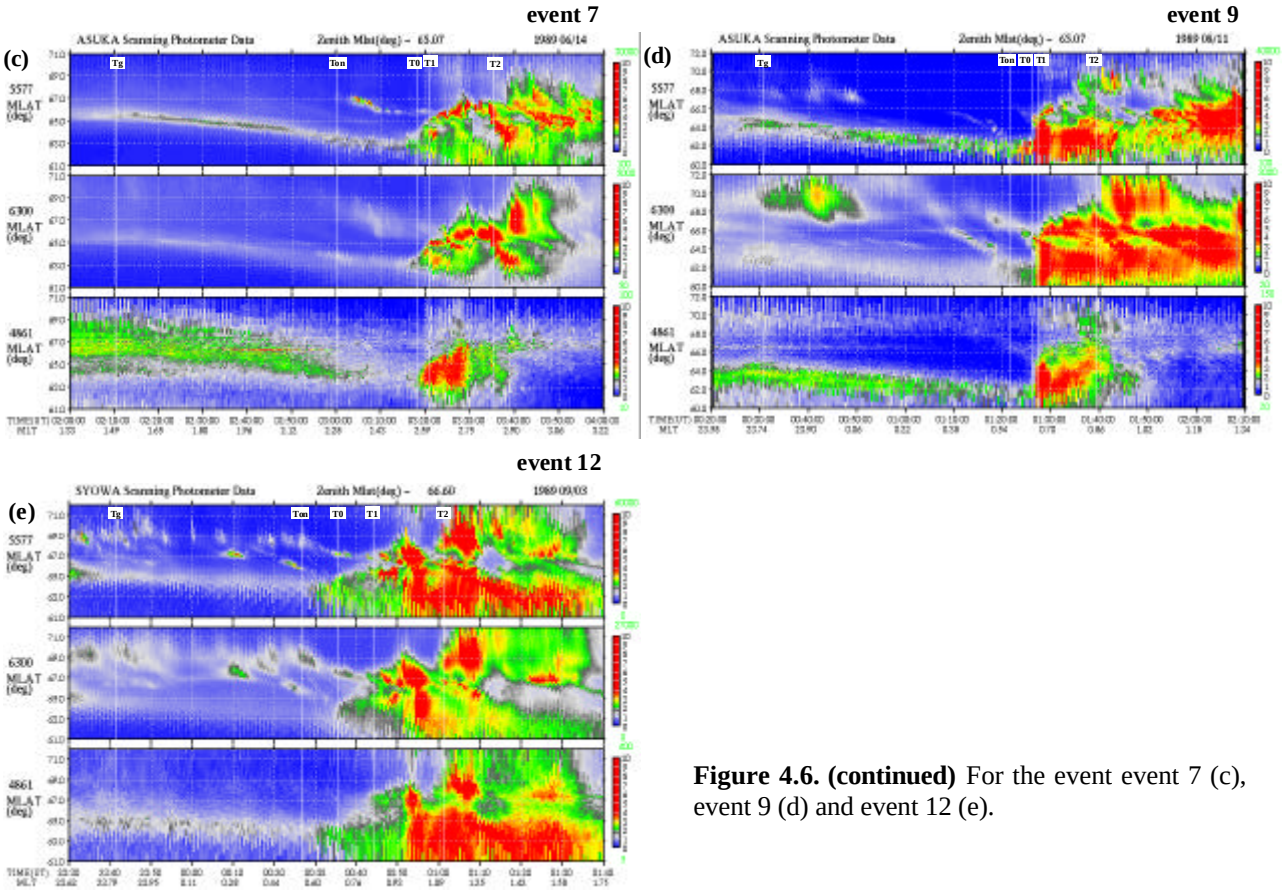

Figure 4.6. (continued) For the event event 7 (c), event 9 (d) and event 12 (e).

The all-sky SIT-TV data are shown in Figure 4.7 for the event 12 (Fig. 4.7(a)) and event 4 (Fig. 4.7(b)). Time advances from the upper left image to the lower right one in each panel.

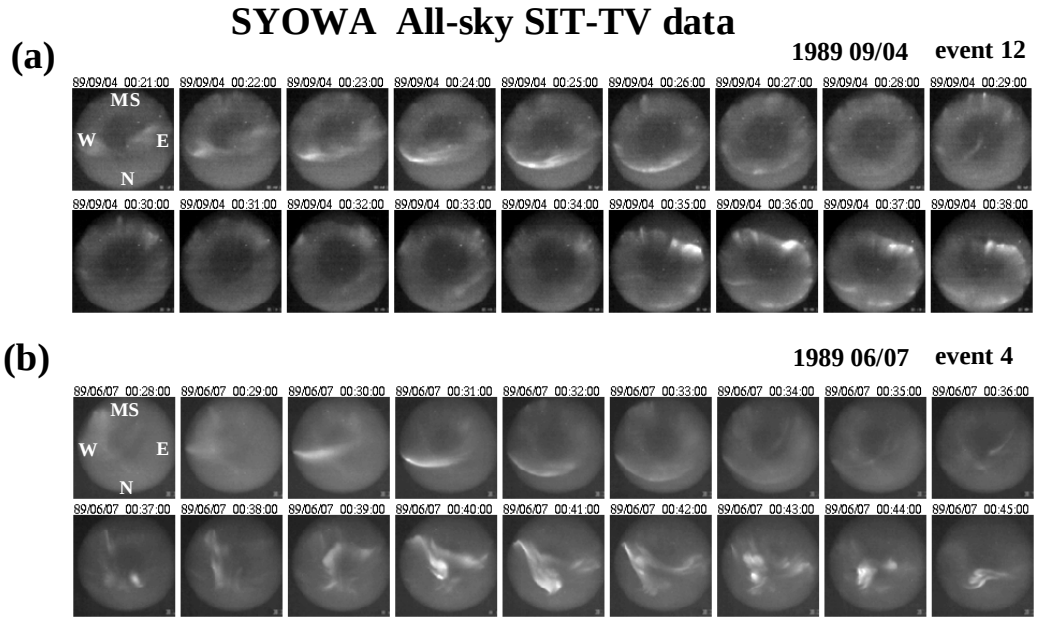

Figure 4.7. All-sky SIT-TV data for the event 12 (a) and event 4 (b) with 1 min interval. In each image, top and right are magnetic poleward and eastward, respectively.

As for the event 12, the FEM arc is clearly identified in the third image in Fig. 4.7(a). Two-dimensional feature of the FEM arc was a longitudinally elongated sharp discrete aurora. It moved equatorward, and its intensity gradually decreased as it moved equatorward. These features of the FEM arc are very similar to those of the FEM arc in the event 4, which can be seen from the third image in Fig. 4.7(b). The NPSBL aurora clearly appeared in the fourth image from the right side in the bottom images in Fig. 4.7(a). It exhibited a ray structure and folds within it. Hence the two-dimensional features of the NPSBL aurora was a little different from those of the FEM arc, as in the case of the event 4, where the NPSBL aurora can be clearly seen in the fourth image from left side in the bottom images in Fig. 4.7(b).

Selected latitudinal intensity profiles during the Stage-1, 2, and 3 are shown in Figure 4.8 for the 6 selected events. In each panel, abscissa is ILAT from 58 to 72 deg, and ordinate is relative emission intensity of the three auroral emission lines. Intensity profiles of the 557.7, 630.0, and 486.1 nm emissions are shown with green, red, and blue lines in each panel, respectively.

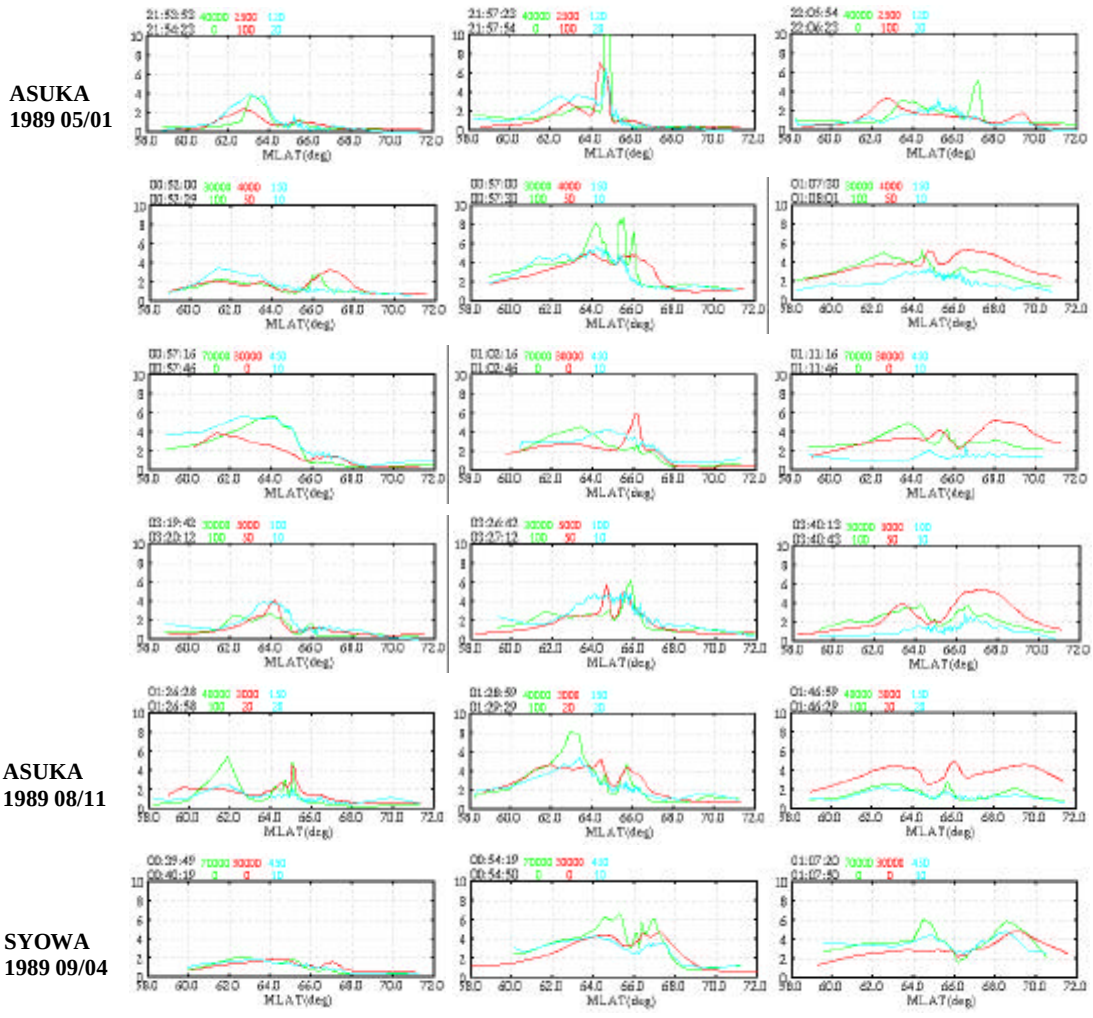

Figure 4.8. Selected latitudinal intensity profiles during the Stage-1, 2, and 3 for the 6 selected events.

During the Stage-1, both electron and proton emissions co-existed in the main auroral region. The NPSBL aurora can be identified as a small bump on the higher latitude side in each panel during the Stage-1. During the Stage-2, an intense electron auroral activity appeared around the interface region between the main auroral region and the NPSBL aurora. Intensity of the NPSBL aurora was also enhanced, except in the event 2, whereas the latitudinal location of the NPSBL did not change significantly. In the main auroral region on the lower latitude side, both the electron and proton auroral emissions co-existed as in the Stage-1. During the Stage-3, the poleward-most auroral region significantly spread poleward and an intensity gap appeared between the poleward region and the electron main auroral region on the equatorward side. The proton auroral emission region also spread poleward. Within the electron main auroral region on the equatorward side, the proton auroral emission was significantly reduced, except in the event 12. The latitudinal intensity profiles for the other 7 events, which are listed in Table 4.2, are shown in Figure 4.9 in same format as in Fig. 4.8. Basically similar features can be seen in those other events.

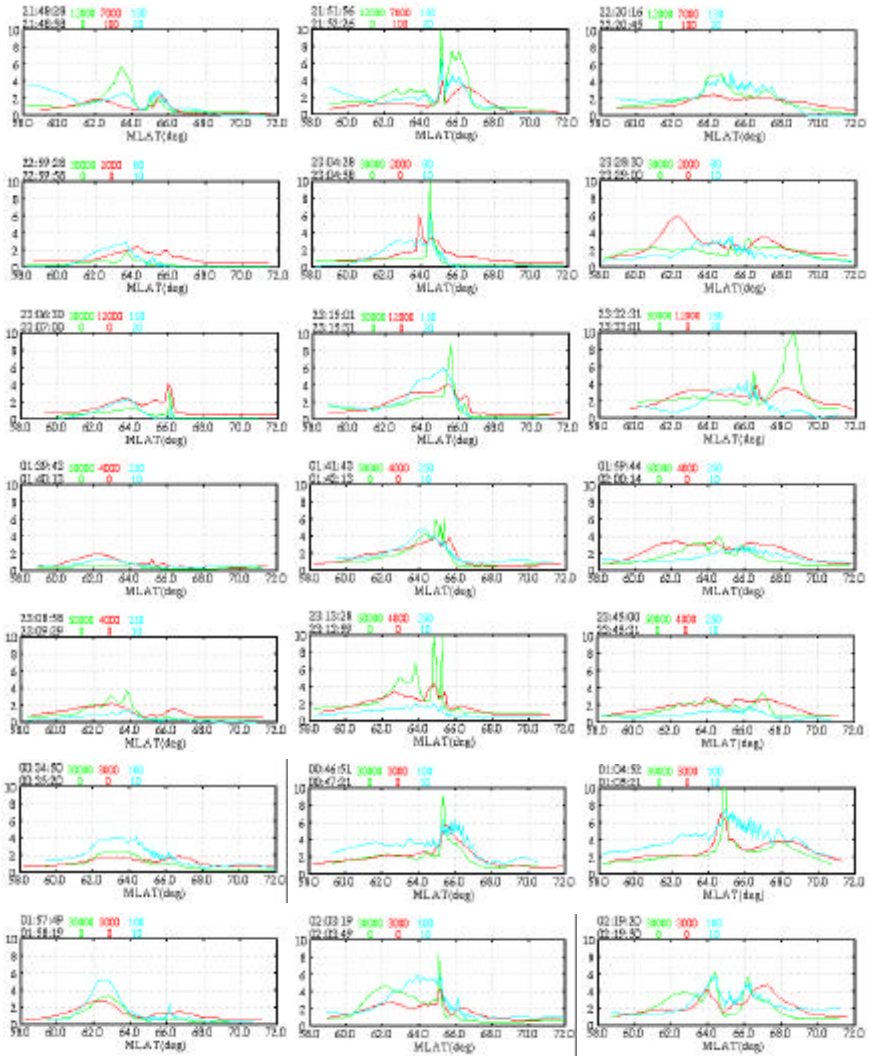

Figure 4.9. Selected latitudinal intensity profiles during the Stage-1, 2, and 3 for the 7 other events.

4.5. Statistical results

Statistical results from the 13 events are shown in Table 4.3. The FEM arc can be identified in the 6 events. In the event 1, transition from the Stage-2 to Stage-3 was less clear. The fading of the proton auroral emission after T2 was observed in the 10 events. Average location of the start of the initial poleward expansion was 23.8 hour in MLT and 62.7 deg in ILAT. Average ceiling latitude of the initial poleward expansion was 64.6 deg, and average duration of the Stage-1 (T1-T0) was 3.3 min. Hence the average speed of the initial poleward expansion was 1.1 km/s. Average latitude of the NPSBL aurora at T0 was 66.4 deg. Hence the initial poleward expansion started at the lower latitudes by 3.7 deg in average from the poleward boundary of the entire auroral region. The Stage-3 started 14.0 min after T0 in average, hence the average duration of the Stage-2 was 10.7 min, which was about three times longer than the duration of the Stage-1. Average duration of the local growth phase was 63.8 min.

Table 4.3. Summary of the MSP observation for the stepwise evolution event in 1989

total no	good event	NPSBL aurora	FEM arc	3 stage evolution	proton fade	MLT0 (hour)	ILAT0 (deg)	ILAT1 (deg)	ILAT NPSBL	T1-T0 (min)	T2-T0 (min)	T0-Tg (min)
88	13 (15%)	13 (100%)	6 (46%)	12 (92%)	10 (77%)	23.8	62.7	64.6	66.4	3.3	14.1	63.8

Figure 4.10 shows the distribution of the start location of the initial poleward expansion for the total 88 events (Fig. 4.10(a)) and for the selected 13 events (Fig. 4.10(b)).

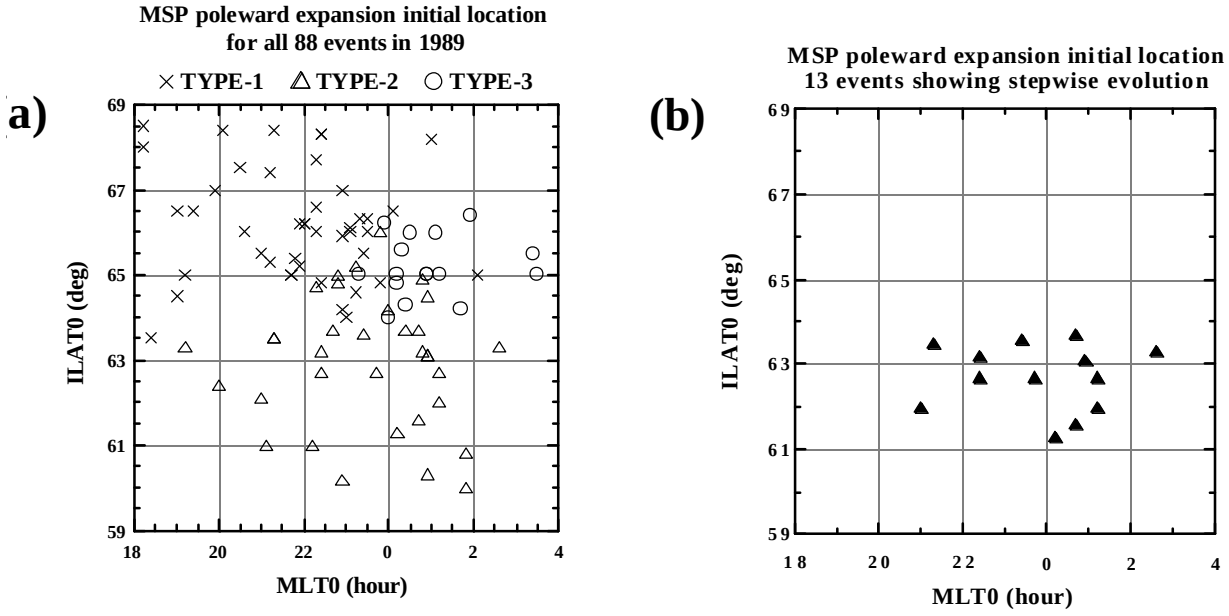

Figure 4.10. Distribution of the start location of the initial poleward expansion for the total 88 events (a) and for the selected 13 events (b). Panel (a) is the same as Fig. 2.8.

It is clear that the initial poleward expansion in the selected events occurred at the lower

latitude region around midnight hours. If we search the "good" event within the range of 20-02 hr MLT and ILAT less than 64.0 deg, then occurrence rate of the "good" event becomes 52 % in the total 25 events. Hence it can be said that the features schematically shown in Fig. 4.1 can be seen with a high probability when the initial poleward expansion starts at such a lower latitude region around midnight hours as mentioned above. On the other hand, the features of the poleward expansion in the higher latitude region and off-midnight hours should be deviated from those shown in Fig. 4.1.

Figure 4.11 shows a relationship between the durations T1-T0 and T2-T1. There seems to be a positive relationship between them. Hence, if the duration of the Stage-1 is short, then the duration of the Stage-2 is short or the Stage-3 tends to start earlier, and vice versa.

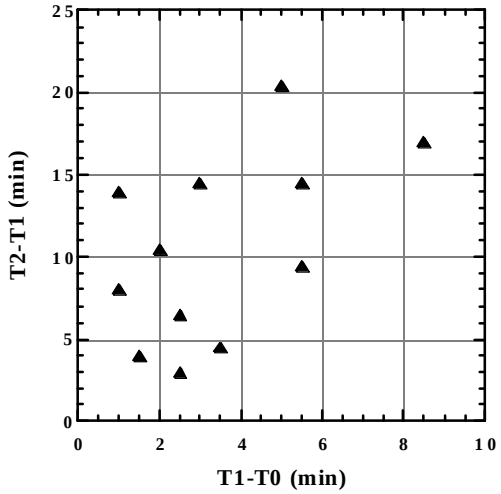

Figure 4.11. Relationship between durations T1-T0 and T2-T1.

4.6. Summary and conclusion of this Chapter

The 13 "good" events were selected from the total 88 poleward expansion events, observed by the MSP at Syowa and Asuka stations in 1989. In those 13 events, we could find the similar features in the auroral substorm evolution as can be seen in the one special event on June 6-7, 1989. The statistical results suggest that such features should appear when the initial poleward expansion occurs at the sufficiently lower latitude region around midnight hours. In the case of a well-developed substorm, the auroral oval expands to lower latitude during the growth phase, and the auroral breakup occurs at the pre-midnight localized region within the well-expanded auroral oval. The observations by the MSP show the local poleward expansion, and in many cases, those expansions occur as a result of the azimuthal expansion of the global auroral bulge. However our result suggests that, in a well-developed substorm, the global auroral bulge evolution should have such features as illustrated by the MSP observation.

The 3-stage stepwise evolution of the auroral poleward expansion and the important role of the NPSBL aurora for the evolution were confirmed with the selected 13 "good" events. These two points should be important when one considers about the evolution of the magnetospheric substorm.